LAPTM4B-35 promotes cancer cell migration via stimulating integrin beta1 recycling and focal adhesion dynamics

Liu, Minxia

2022-06

ORIGINAL ARTICLE

Cancer Science WILEY

LAPTM4B-35 promotes cancer cell migration via stimulating integrin beta1 recycling and focal adhesion dynamics

Minxia Liu[1,2] | Ruyu Yan[1] | Junjie Wang[1] | Zhihong Yao[3] | Xinyu Fan[4] |
Kecheng Zhou[1,5,6] 🔟

[1]School of Life Science, Anhui Medical University, Hefei, China

[2]Institute for Molecular Medicine Finland, Helsinki Institute of Life Science, University of Helsinki, Helsinki, Finland

[3]Department of Orthopaedics, The Third Affiliated Hospital of Kunming Medical University (YunnanCancer Hospital), Kunming, China

[4]Department of Orthopaedic Surgery, 920th Hospital of Joint Logistics Support Force, Kunming, China

[5]Faculty of Medicine, Department of Anatomy, University of Helsinki, Helsinki, Finland

[6]Minerva Foundation Institute for Medical Research, Helsinki, Finland

Correspondence
Kecheng Zhou, Group Leader of "Cancer Metabolism Laboratory," School of Life Science, Anhui Medical University, 81 Meishan Road, 230032, Hefei, Anhui, China.
Email: zhoukecheng@ahmu.edu.cn

Abstract

Metastasis is the main cause of cancer patients' death despite tremendous efforts invested in developing the related molecular mechanisms. During cancer cell migration, cells undergo dynamic regulation of filopodia, focal adhesion, and endosome trafficking. Cdc42 is imperative for maintaining cell morphology and filopodia, regulating cell movement. Integrin beta1 activates on the endosome, the majority of which distributes itself on the plasma membrane, indicating that endocytic trafficking is essential for this activity. In cancers, high expression of lysosome-associated protein transmembrane 4B (LAPTM4B) is associated with poor prognosis. LAPTM4B-35 has been reported as displaying plasma membrane distribution and being associated with cancer cell migration. However, the detailed mechanism of its isoform-specific distribution and whether it relates to cell migration remain unknown. Here, we first report and quantify the filopodia localization of LAPTM4B-35: mechanically, that specific interaction with Cdc42 promoted its localization to the filopodia. Furthermore, our data show that LAPTM4B-35 stabilized filopodia and regulated integrin beta1 recycling via interaction and cotrafficking on the endosome. In our zebrafish xenograft model, LAPTM4B-35 stimulated the formation and dynamics of focal adhesion, further promoting cancer cell dissemination, whereas in skin cancer patients, LAPTM4B level correlated with poor prognosis. In short, this study establishes an insight into the mechanism of LAPTM4B-35 filopodia distribution, as well as into its biological effects and its clinical significance, providing a novel target for cancer therapeutics development.

KEYWORDS
Cdc42, filopodia, focal adhesion, integrin beta1 recycling, LAPTM4B-35

---

1 | INTRODUCTION

As one of the cancer hallmarks,[1] metastasis leads to most treatment failure and cancer mortality.[2] Metastatic dissemination induces poor prognosis in current cancer treatment and represents the truly malignant character of cancers. Huge progress has occurred in uncovering the details of the metastatic mechanism, but its sophisticated signal transduction and molecular regulation demand further investigation.

Cancer cell migration is a multistep process with the involvement of multiple organelles. Filopodia, cell protrusion which is the elongation of actin, sensing extracellular nutrients and signals, usually points in the direction of cell movement under regulation by a GTPase such as Cdc42.[3-5] Focal adhesion (FA), large macromolecular assemblies which anchor the extracellular matrix to the cytoskeleton and mediate cell-matrix adhesion, requires structural and regulatory proteins including integrin.[6,7] Focal adhesion formation and dynamics are imperative for cancer cell migration.[7] During the directed cell migration, endocytic trafficking is fundamental for maintaining the molecular signal and substance transportation, regulating integrin activity and FA dynamics.[8,9]

The late endosomal protein, LAPTM4B, was first identified from a transcript that is upregulated in hepatocellular carcinoma.[10] Initial characterizations suggested that the mRNA is translated to a 35-kDa protein isoform (LAPTM4B-35) and an alternative 24-kDa isoform (LAPTM4B-24) that lacks 91N-terminal amino acids.[10] Subsequent studies have linked high LAPTM4B expression to poor prognosis in several cancers, including myeloid leukemia,[11] breast cancer,[12] and hepatocellular carcinoma.[13] LAPTM4B-35 has been associated with epithelial-mesenchymal transition,[14,15] cell migration, invasion,[16] and metastasis.[17] LAPTM4B expression causes an increase in actin-based plasma membrane protrusions,[18] structures known to be critical in directed cell migration.[3] Part of the migratory phenotype may be mediated by the SH3 domain binding motif in the N-terminus of LAPTM4B-35.[16]

We have found that LAPTM4B interacts with ceramide, regulating lysosomal leucine update and the downstream mTORC1 activity.[19] We further showed LAPTM4B isoforms display a distinct distribution, with both isoforms localized on the endosome. LAPTM4B-35 shows, in addition, plasma membrane distribution.[20] Details of the mechanism of isoform-specific distribution and whether it is related to LAPTM4B-35 gain-of-function in cancers are, however, unknown.

In this study, we established that Cdc42 can interact with LAPTM4B-35, which regulates its specific distribution to the filopodia and stabilizes filopodia. Furthermore, LAPTM4B-35 interacted with integrin beta1, promoting its recycling via endosome trafficking. As a cellular result, LAPTM4B-35 regulated downstream FA formation and dynamics. In line with this, we provided evidence that LAPTM4B-35 promotes cancer cell dissemination in a zebrafish model; LAPTM4B correlated with poor prognosis in skin cancer patients. Collectively, this study presented more insights into the mechanism of LAPTM4B-35 distribution and its cellular promigratory phenotype, as well as into its clinical significance as a potential target for cancer therapeutics discovery.

2 | MATERIALS AND METHODS

2.1 | Human cell lines and tissue specimens

A431 cells (ATCC, Cat#CRL-1555) were maintained in Dulbecco's modified Eagle's medium containing 10% fetal bovine serum (FBS), 2 mM L-glutamine, and penicillin/streptomycin (each 100 U/ml). PC-3 (ATCC, Cat#CRL-1435) cells were maintained in ATCC-formulated F-12K medium containing 10% FBS, 2 mM L-glutamine, and penicillin/streptomycin (each 100 U/ml). All cells were grown at 37°C and with 5% CO_2.

Skin cancer tissues came from five patients undergoing resection. No patients had undergone treatment before the surgery. The tumor samples were from primary tumors. All of these samples were diagnosed according to the World Health Organization's classification. Our study was approved by the local research ethics committee.

2.2 | Reagents, plasmids, antibodies, and siRNAs

Celltracker CM-Dil was from Invitrogen (Cat#C7000), Alexa Fluor 568 Phalloidin from Molecular Probes (Cat# A-12380), and X-tremeGENE HP DNA transfection reagent from Sigma (Cat #06366236001). The mouse monoclonal anti-Flag (M2) was from Sigma-Aldrich (Cat#F1804), mouse monoclonal anti-LAPTM4B from Atlas Antibodies (Cat#AMAb91356), anti-Cdc42 from ThermoFisher Scientific (Cat#1862345) provided in the "Active Cdc42 Pull-down and Detection Kit" (Cat#16119), mouse monoclonal anti-pFAK from BD Transduction laboratories (Cat#611807), mouse monoclonal anti-integrin beta1 (total, N29) from Millipore (Cat#MAB2252), and anti-integrin beta1 (active epitope, 9EG7) from BD Pharmingen (Cat#550531). The secondary antibodies goat anti-mouse IgG (H+L)-HRP conjugate was from BioRad (Cat#1706516) and cross-adsorbed Alexa Fluor 488 from ThermoFisher Scientific (Cat#A-11001). The predesigned "Silencer Select" LAPTM4B siRNA (GGAUCAGUAUAACUUUUCATT) was from Ambion. Cdc42 siRNA (ID: VHS40396) and its Ctrl siRNA (ID: 12935300) were Stealth RNAi™ siRNAs, ordered from ThermoFisher Scientific. The plasmids Cdc42[G12V]-EGFP and Cdc42[T17N]-EGFP have been described previously,[21] and GFP-paxillin was a gift from Pekka Lappalainen. The plasmid mCherry-Integrin-Beta1-N-18 was a gift from Michael Davidson (Addgene, Cat#55064).

2.3 | Statistical analysis

All data are presented as mean ± standard error of the mean (SEM) from at least three independent experiments. Statistical significance was based on Student's t test for pairwise comparisons, and Holm's

t test for multiple comparisons. The level of statistical significance was set at 0.05. * indicates $p < 0.05$; *** indicates $p < 0.01$.

Additional detailed descriptions of methods are in Method S1.

3 | RESULTS

3.1 | LAPTM4B-35 localized on filopodia

We have shown LAPTM4B isoforms to display a distinct distribution, both isoforms localized on endosomes; LAPTM4B-35, however, displays additional plasma membrane distribution and has undergone upregulation in several cancer patients' samples.[20] By utilizing the isoform-expressing cells from a knockout (KO) background which we established in a previous study,[20] we firstly measured protein expression level and cell migration. LAPTM4B-35–expressing cells display much higher migratory ability than LAPTM4B-24–expressing cells, even though the protein expression levels are comparable (Figure S1A,B), consistent with our previous finding.[20] To further confirm the effect is not dependent on protein expression level, we generated more cell lines with higher LAPTM4B-24 level and found LAPTM4B-24 displays no effect on cell migration (Figure S2A,B). These data indicate that LAPTM4B isoforms' effect on cell migration is independent of protein expression level.

We noted that in phalloidin-positive cell protrusions, LAPTM4B-35 positive endosomes were abundant (Figure 1A). Data quantification showed LAPTM4B-35 to display a preferential localization to filopodia (Figure 1B), whereas in cells expressing LAPTM4B-35 compared with those expressing LAPTM4B-24, the total numbers of actin-based protrusions per cell did not differ (Figure 1C). Additionally, by employing live-cell imaging, we found that LAPTM4B-35-mCherry–positive endosomes moved toward the filopodia tips (Video S1), similarly to those in the confocal images (Figure 1A). In contrast, LAPTM4B-24 was less prominent in plasma membrane protrusions (Figure 1A,B), suggesting that LAPTM4B-35 may have gained certain cell protrusion–related functions.

3.2 | LAPTM4B-35 interacted with Cdc42 and promotes filopodia stabilization

Filopodia are essential for cell movement, and Cdc42 is a known inducer of filopodia[22]; we therefore next investigated whether Cdc42 is functionally connected with LAPTM4B. Coimmunoprecipitation experiments revealed LAPTM4B-35 to interact with both constitutively active Cdc42^{G12V} (Figure 2A) and the dominant negative Cdc42^{T17N} (Figure 2B), whereas LAPTM4B-24 showed no interaction with either of these Cdc42 forms (Figure 2A,B). The specificity of the protein-protein interaction was further confirmed by immunoprecipitation of endogenous LAPTM4B, using Cdc42-GFP as a bait. In these experiments, LAPTM4B-35 displayed a ~4-fold enrichment over LAPTM4B-24 (Figure 2C), suggesting a preferred interaction between LAPTM4B-35 and Cdc42. Interestingly, immunoprecipitation of active endogenous Cdc42 with the Pak1-binding domain revealed that LAPTM4B did not
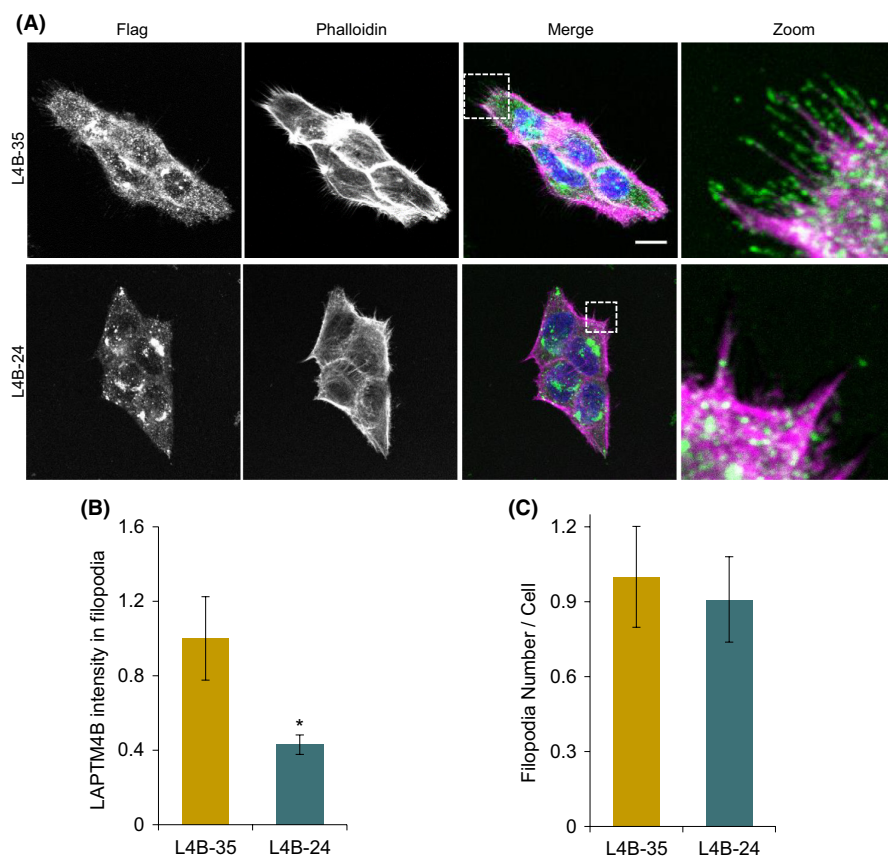

FIGURE 1 LAPTM4B-35 localized on filopodia. (A), LAPTM4B KO cells stably expressing LAPTM4B-35-Flag (designated name in this study: L4B-35) or LAPTM4B-24-Flag (designated name in this study: L4B-24) were labeled with anti-Flag antibody (green), phalloidin-568 (magenta), and DAPI (blue). Scale bar: 10 μm. (B), Quantification of LAPTM4B immunofluorescence intensity in phalloidin-positive filopodia. Quantification of three experiments (LAPTM4B-35: $n = 41$ cells; LAPTM4B-24: $n = 43$ cells), mean ± SEM, data normalized to "L4B-35," $p = 0.015$. (C), Number of filopodia in cells stably expressing Flag-tagged LAPTM4B-35 or LAPTM4B-24 on a LAPTM4B KO background. Quantification of three experiments (LAPTM4B-35: $n = 41$ cells; LAPTM4B-24: $n = 43$ cells), mean ± SEM, data normalized to "L4B-35"
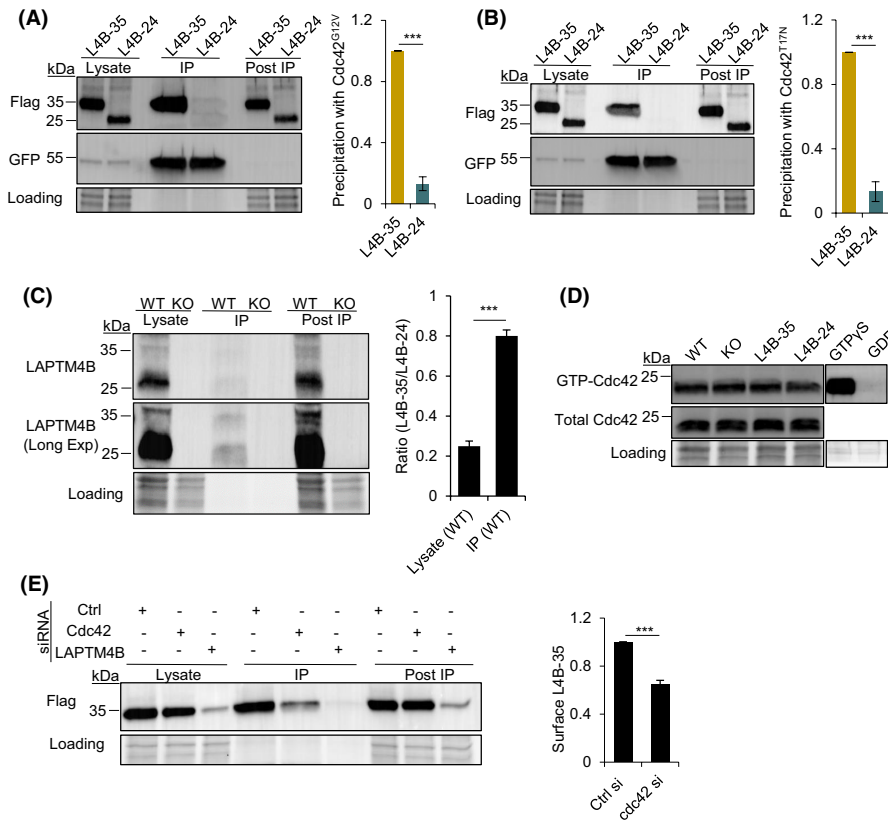
FIGURE 2 Cdc42 required for LAPTM4B-35 surface localization. (A), LAPTM4B KO cells stably expressing Flag-tagged LAPTM4B-35 or LAPTM4B-24 were transfected with constitutively active Cdc42^{G12V}-GFP. The Cdc42^{G12V}-GFP was pulled down using GFP-trap, with coimmunoprecipitated LAPTM4B, and then detected by Western blotting. The blot was reprobed with GFP antibody. Left panel: representative experiment. Right panel: quantification of $n = 3$ experiments, mean $\pm$ SEM, data normalized to "L4B-35," $p = 9.87 \times 10^{-5}$. "Lysate" denotes total cell lysate, "IP" the immunoprecipitated protein, and "post IP" the remaining supernatant after immunoprecipitation. (B), Cells stably expressing LAPTM4B-35 and LAPTM4B-24 were transfected with the dominant negative Cdc^{T17N}-GFP. The Cdc42^{T17N}-GFP was pulled down using GFP-trap, and its interaction with the LAPTM4B isoforms was assessed by Western blotting. Left panel: a representative experiment. Right panel: quantification of three experiments, mean $\pm$ SEM, data normalized to "L4B-35." $p = 0.0003$. (C), Coimmunoprecipitation of endogenous LAPTM4B with Cdc^{G12V}-GFP from WT A431 cells. LAPTM4B KO cells served as a control for antibody specificity. The Cdc42-GFP was pulled down using GFP-trap, and the interaction was further assessed by Western blotting using anti-LAPTM4B antibody. Left panel: a representative experiment. Right panel: quantification of three experiments, mean $\pm$ SEM, $p = 5.09 \times 10^{-5}$. D, Whole-cell lysates were assessed for active Cdc42. Lysates treated with GTPγS or with GDP served as the positive and negative control. E, Plasma-membrane expression of LAPTM4B-35 was assessed by surface biotinylation in cells stably expressing LAPTM4B-35-Flag, treated with control, Cdc42, or LAPTM4B siRNAs, followed by Western blotting using anti-Flag antibody. Left panel: representative experiment. Right panel: quantification of three experiments, mean $\pm$ SEM, data normalized to "Ctrl siRNA," $p = 0.0009$

affect cellular Cdc42 activity (Figure 2D). We therefore hypothesized that Cdc42 may instead regulate LAPTM4B localization and function.

Surface biotinylation experiments revealed that Cdc42-depleted cells had significantly reduced LAPTM4B-35 levels on the plasma membrane (Figure 2E, Figure S3A). In line with this observation, filopodia induced by expression of the constitutively active Cdc42^{G12V} were strongly positive for LAPTM4B-35 (Figure 3A; Video S2). Instead, in cells where filopodia formation was suppressed by expression of the dominant negative Cdc42^{T17N}, LAPTM4B-35 positive endosomes accumulated in the cell periphery close to plasma membrane protrusions (Figure 3B, Video S3). These findings from live-cell imaging were supported by the images in fixed cells (Figure S3B).

Stable filopodia are necessary for sensing extracellular environment and directed migration.[23] Accordingly, we observed

constitutively active Cdc42^{G12V}-expressing cells to contain more stabilized filopodia as measured by filopodia tip movement (Figure 3C). We next assessed whether LAPTM4B-35 expression was associated with filopodia dynamics. Interestingly, quantification of live-cell images revealed that filopodia were more stable in LAPTM4B-35–expressing cells (Figure 3D).

3.3 | LAPTM4B-35 stimulated FA formation and dynamics

Filopodia stabilization precedes the maturation of FAs, which is an early event of directed cell migration.[3,24] Hence, we assessed whether LAPTM4B-35 regulates FA formation and dynamics. Immunofluorescence staining showed that p-FAK positive FAs
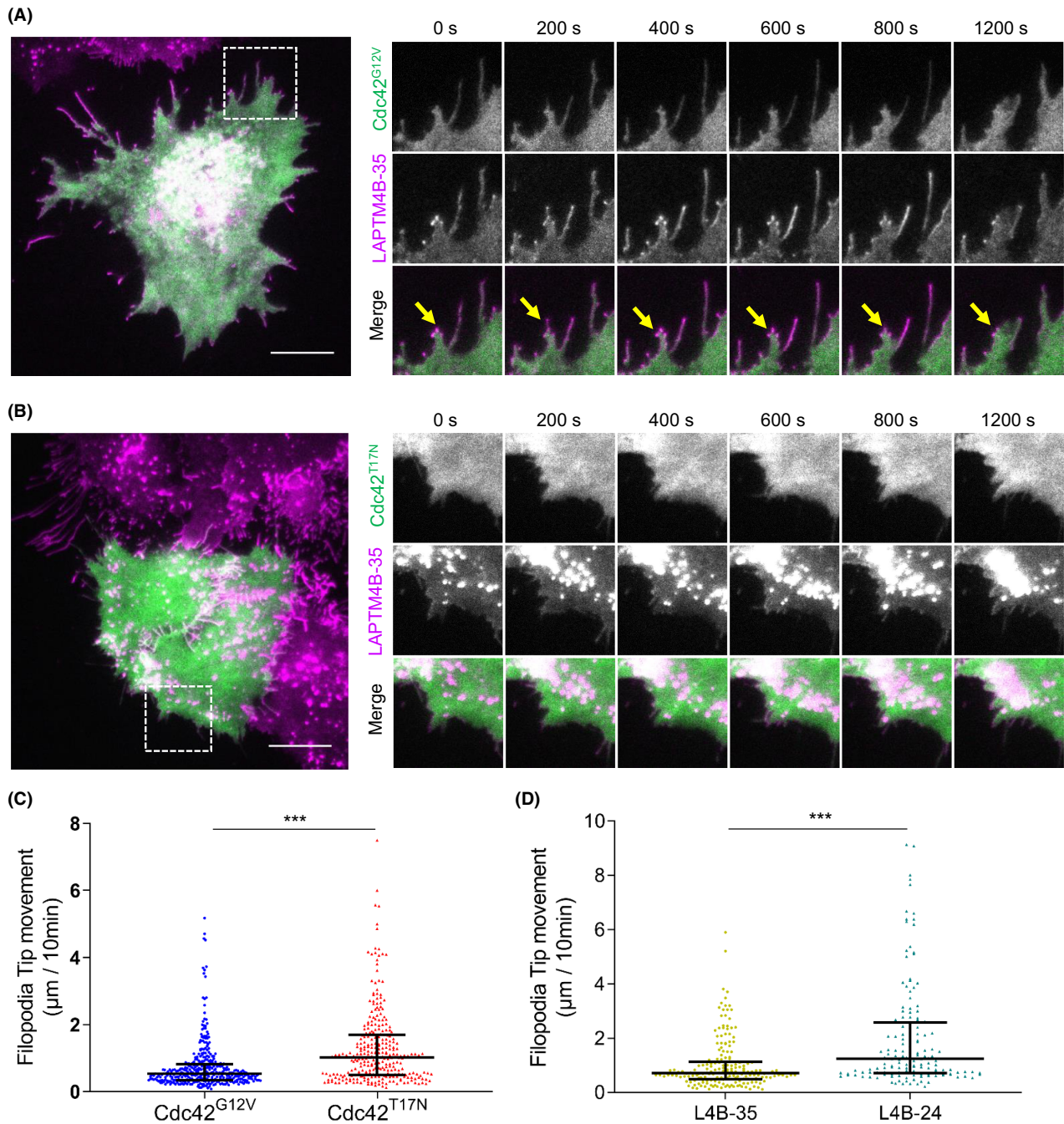
FIGURE 3 LAPTM4B-35 distributing on Cdc42-induced filopodia. A, A431 cells stably expressing LAPTM4B-35-mCherry were transiently transfected with constitutively active Cdc42^{G12V}-GFP and imaged by live total internal reflection fluorescence (TIRF) microscopy. Scale bar: 10 μm. A magnified region of interest at different time points is visible on the right. Yellow arrows highlight LAPTM4B-35 positive filopodia. B, A431 cells stably expressing LAPTM4B-35-mCherry were transiently transfected with dominant negative Cdc42^{T17N}-GFP, and imaged by TIRF microscopy. Scale bar: 10 μm. A region of interest at different time points is on the right. C, A431 cells stably expressing LAPTM4B-35-mCherry were transiently transfected with either constitutively active Cdc42^{G12V}-GFP or dominant negative Cdc42^{T17N}-GFP and imaged by TIRF microscopy. The distance of filopodia tip movement in 10 min was quantified. Each dot represents a single measurement, middle line represents mean, and whiskers represent interquartile range. D, Cells stably expressing Flag-tagged LAPTM4B-35 and LAPTM4B-24 were transfected with integrin beta1-mCherry to visualize cell protrusions, and cells were imaged by live TIRF microscopy. The distance of filopodia tip movement in 10 min was quantified. Data are from three independent experiments and >10 videos per condition. LAPTM4B-35: $n = 196$ filopodia; LAPTM4B-24: $n = 151$ filopodia; $p = 8.8 \times 10^{-8}$. Each dot represents a single measurement, middle line represents mean, and whiskers represent interquartile range
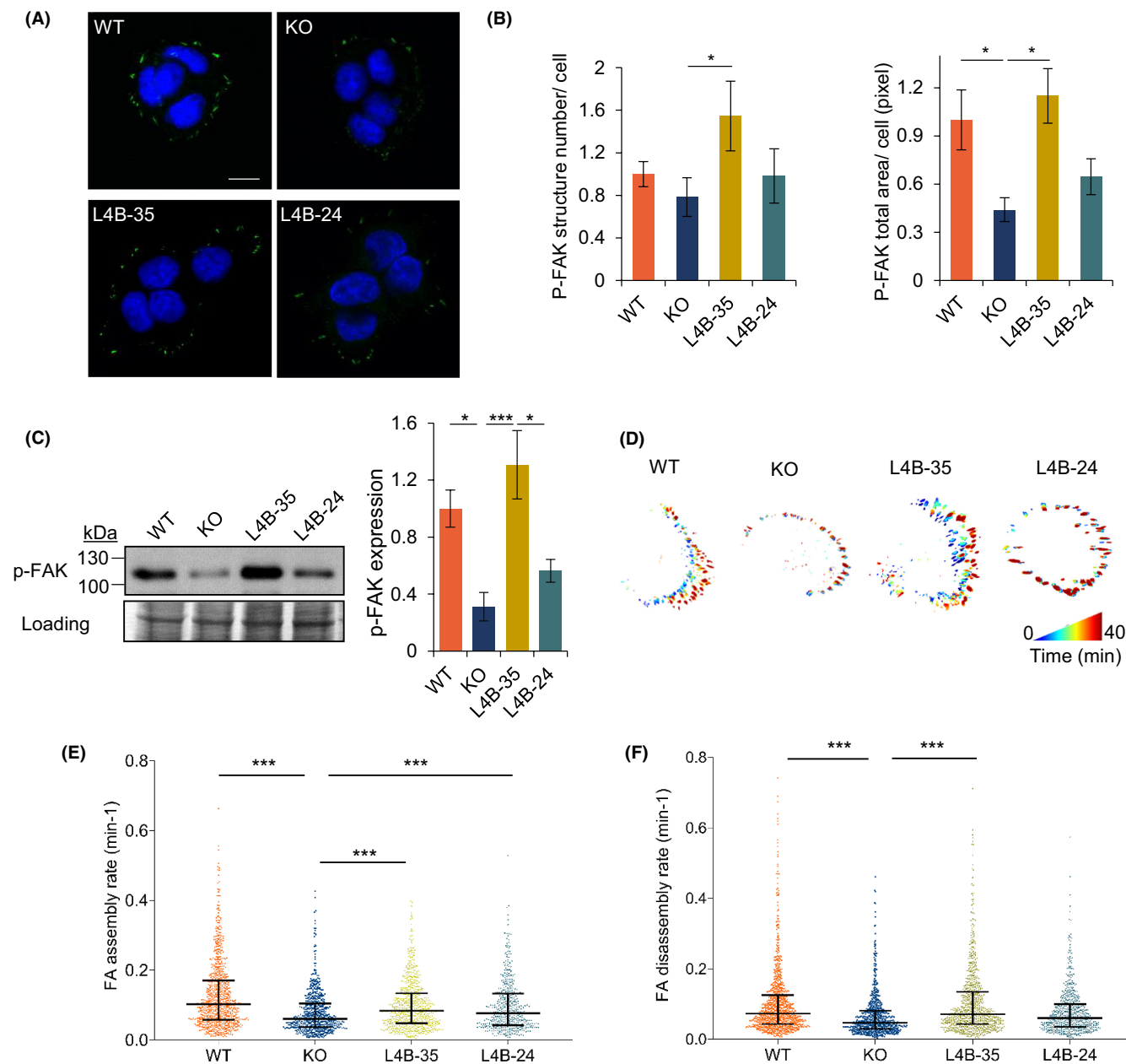
FIGURE 4 LAPTM4B-35 stimulating focal adhesion formation and dynamics. A, Immunofluorescence staining of p-FAK–positive focal adhesions in A431 WT, LAPTM4B KO, and cells expressing LAPTM4B-24 or LAPTM4B-35 on the KO background. Scale bar: 10 μm. B, Quantification of the number (left panel, p[KO, L4B-35] = 0.022) and area (right panel, p[WT, KO] = 0.017, p[KO, L4B-35] = 0.016) of p-FAK–positive structures in WT, LAPTM4B KO, LAPTM4B-24, and LAPTM4B-35 cells. Data from three independent experiments, WT: n = 40 cells, KO: n = 38 cells; LAPTM4B-35: n = 40 cells; LAPTM4B-24: n = 44 cells. Mean ± SEM, data normalized to "WT." C, Western blotting shows total cellular p-FAK expression in A431 WT, LAPTM4B KO, and KO cells with reintroduction of the indicated LAPTM4B isoforms. Left panel: a representative experiment. Right panel: quantification of three experiments, mean ± SEM, p(WT, KO) = 0.032, p(KO, LAPTM4B-35) = 0.008, p(LAPTM4B-35, LAPTM4B-24) = 0.027. D, WT, LAPTM4B KO, or A431 cells stably expressing LAPTM4B-24 or LAPTM4B-35 were transfected with paxillin-GFP to label focal adhesions. Paxillin-GFP dynamics were assessed by total internal reflection fluorescence (TIRF) microscopy and subjected to automated quantification. A representative visualization of focal adhesion dynamics over 40 min is shown (blue indicates the start point of imaging, while red indicates the end point of imaging). E, Focal adhesion (FA) assembly rate (min^{-1}) in the indicated cell lines treated as in (D). p(WT, KO) = 4.5 × 10^{-30}, p(KO, LAPTM4B-35) = 1.29 × 10^{-8}, p(KO, LAPTM4B-24) = 2.85 × 10^{-5}. The data are from five independent experiments, and >18 videos per condition. Number of adhesions analyzed; WT: n = 858, KO: n = 646; LAPTM4B-35: n = 752; LAPTM4B-24: n = 504. Each dot represents a single measurement, middle line represents mean, and whiskers represent interquartile range. F, Focal adhesion (FA) disassembly rate (min^{-1}) in WT, LAPTM4B-KO, LAPTM4B-24, and LAPTM4B-35 cell lines. p(WT, KO) = 2.4 × 10^{-21}, p(KO, LAPTM4B-35) = 1.6 × 10^{-20}. The data are from five independent experiments and >18 videos per condition. Number of adhesions analyzed, WT: n = 1025; KO: n = 732; LAPTM4B-35: n = 859; LAPTM4B-24: n = 628
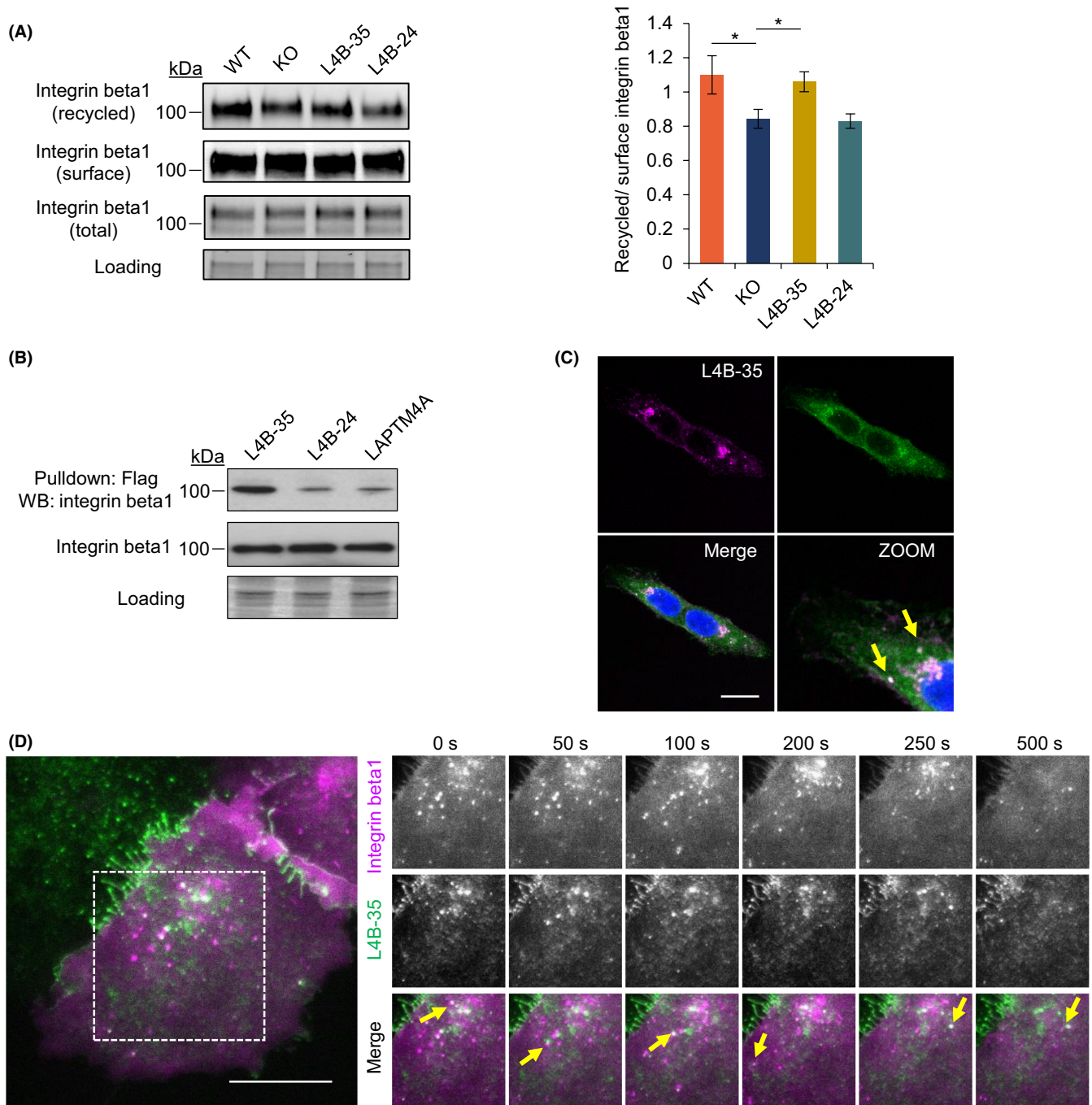
FIGURE 5 LAPTM4B-35 promoting recycling of integrin beta1. A, Western blotting shows recycled integrin beta1 to be reduced in KO cells and rescuable by LAPTM4B-35 expression. Left panel: a representative experiment. Right panel: quantification of three experiments, mean ± SEM, p(WT, KO) = 0.044, p(KO, LAPTM4B-35) = 0.024. B, LAPTM4B KO cells stably expressing LAPTM4B-35-Flag or LAPTM4B-24-Flag, together with A431-expressing LAPTM4A-Flag cells, were pulled down via anti-Flag antibody; coimmunoprecipitated integrin beta1 detected by Western blotting. C, A431 cells stably expressing LAPTM4B-35-mCherry were stained with anti-integrin beta1(N29) antibody. Confocal microscopy revealed the colocalizations to be on the endosome. Scale bar: 10 μm. Yellow arrows highlight the colocalization. D, A431 cells stably expressing LAPTM4B-35-GFP were transiently transfected with integrin beta1-mCherry and imaged by live TIRF microscopy. Scale bar: 10 μm. A magnified region of interest at different time points is displayed on the right. Yellow arrows highlight the colocalization

were reduced in LAPTM4B KO cells, and that this phenotype was rescued by LAPTM4B-35 but not by LAPTM4B-24 (Figure 4A,B), albeit the individual area of p-FAK structure was not altered by LAPTM4B (Figure S4). Western blotting further suggested that

total cellular p-FAK was increased by LAPTM4B-35 (Figure 4C). To monitor LAPTM4B-mediated regulation of FA dynamics, we performed live-cell total internal reflection fluorescence (TIRF) microscopy of cells expressing GFP-paxillin as an FA marker (Figure 4D,
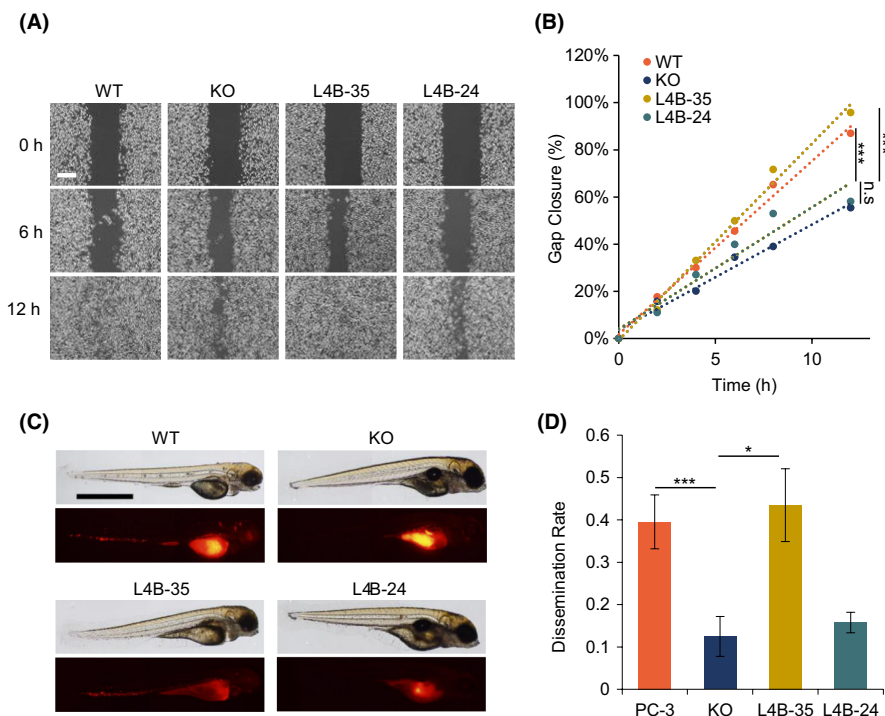
(A)

(B)

(C)

(D)

FIGURE 6 LAPTM4B-35 promoting cancer cell dissemination. A, WT, LAPTM4B KO, and LAPTM4B-24– or LAPTM4B-35–stably expressing PC-3 cells were subjected to a wound-healing assay. Images are representative of five independent experiments at indicated time points. Scale bar: 200 μm. B, Quantification of wound closure of cells treated as in (A). Values represent the average of five experiments, showing percentage of gap closure at indicated times. C, WT, LAPTM4B KO, and LAPTM4B-24– or LAPTM4B-35–stably expressing PC-3 cells were labeled with Celltracker CM-DiI and injected into the perivitelline cavity of WT zebrafish embryos 48 h post fertilization; 36 h post injection, zebrafish were anesthetized and imaged. Cells dissemination from the perivitelline cavity throughout the fish body underwent assessment. Scale bar: 1 mm. D, Metastasis rate of PC-3 cells in zebrafish (fish number with metastases/total fish number). Five independent experiments (PC-3: $n = 43$; KO: $n = 48$; LAPTM4B-35: $n = 46$; LAPTM4B-24: $n = 57$), p(PC-3, KO) = 0.003, p(KO, LAPTM4B-35) = 0.014

Video S4). In comparison with wild-type (WT) cells, LAPTM4B KO cells displayed lower rates of FA assembly (Figure 4E) and disassembly (Figure 4F). Interestingly, the FA disassembly rate can be only rescued by LAPTM4B-35 (Figure 4F). Moreover, the FA lifetime is not altered by LAPTM4B (Figure S5). As FA lifetime/life cycle incudes FA assembly, FA disassembly, and the stability time,[25] our data suggest LAPTM4B may also affect the stability time of FA. In summary, our biochemical data and live-cell imaging experiments indicate that LAPTM4B-35 displays stimulation on FA formation and dynamics.

3.4 | LAPTM4B-35 promoted the recycling of integrin beta1

The integrin-containing filopodia are critical for cell sensing and migration.[7] Furthermore, as one of the major components of FA, the trafficking of integrin beta1 (especially the recycling) is crucial for cell migration and FA turnover.[6,26-28] We thus questioned whether LAPTM4B affects the recycling of integrin beta1. Here, we utilized a Biotin-IP–based method, as described previously.[29] Our data show that LAPTM4B KO cells display moderately less recycled integrin beta1 than do WT cells. Furthermore, this reduced recycling can be rescued by LAPTM4B-35 (Figure 5A).

We further investigated how LAPTM4B-35 regulates the integrin beta1 recycling process. Protein immunoprecipitation results show that LAPTM4B-35 interacts with integrin beta1 (Figure 5B). Meanwhile, confocal experiments report that LAPTM4B-35 colocalizes with integrin beta1 on the endosome (Figure 5C). We next employed live-cell imaging techniques to visualize the intracellular trafficking. Intriguingly, our data showed how a portion of integrin beta1 trafficked via the LAPTM4B-35–positive endosome (Figure 5D, Video S5). Herein, our studies from biochemistry and imaging established that LAPTM4B-35 can promote integrin beta1 recycling via regulation of its endosome trafficking.

3.5 | LAPTM4B-35 regulated cancer cell dissemination

We and others have shown LAPTM4B-35 promotes cancer cell migration in vitro.[15,20,30] Several studies show that LAPTM4B-35 fosters cancer cell metastasis in vivo by utilizing cells overexpressing LAPTM4B-35 in a WT background.[17,31] Here, to further determine the effect of LAPTM4B in cancer cell dissemination, we used an established zebrafish xenograft model.[32,33] As the PC-3 cell line contains a high ability to metastasize and has been used in a zebrafish xenograft model,[32] and the A431 cell line had not been used in
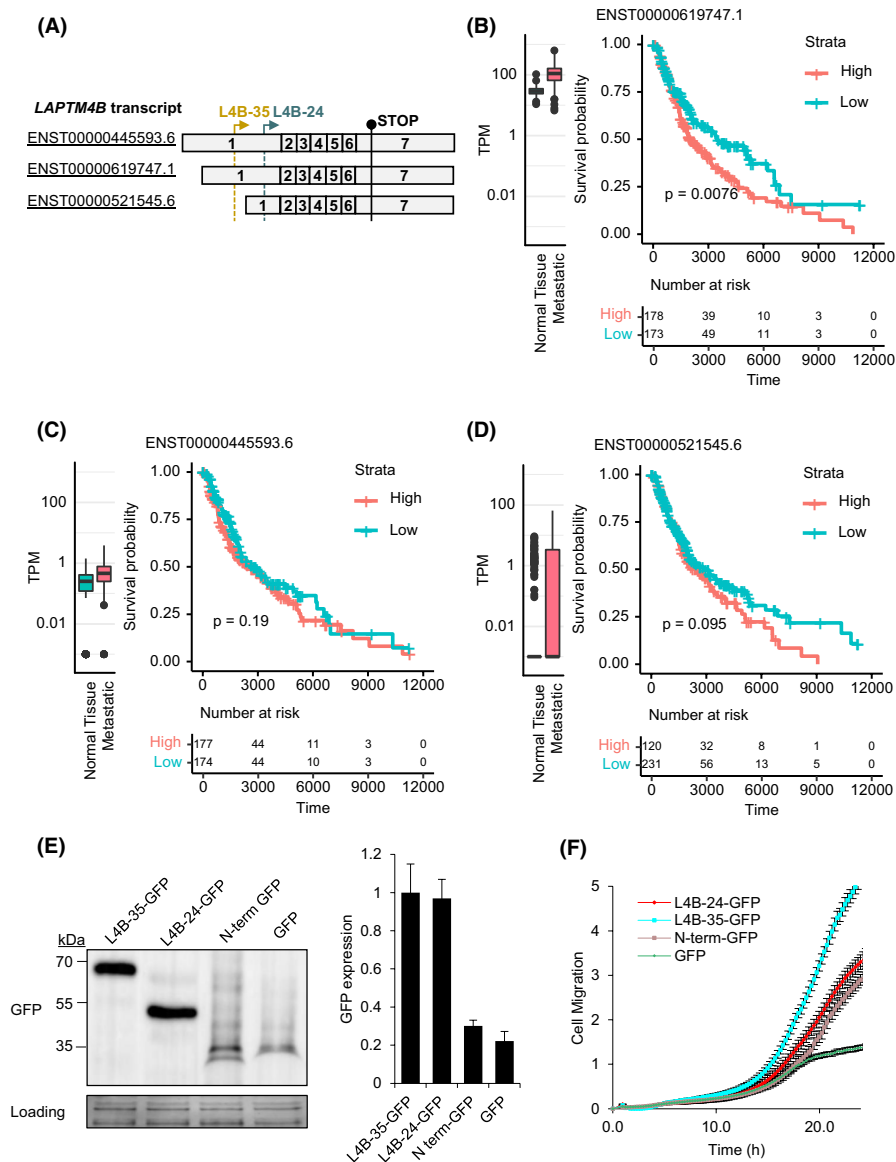
FIGURE 7 LAPTM4B expression correlates with survival probability in skin cancer metastatic patients. A, Schematic overview of the LAPTM4B transcripts. B-D, Expression of the indicated LAPTM4B transcripts in healthy and tumor samples, and their correlation with cancer overall survival. Left panels: expression of the transcript as transcripts per million (TPM) in normal skin (GTEx) and skin cancer metastatic tissues (TCGA), $\log^{10}$ scale. Right panels: skin cancer metastatic patient survival probability with patients grouped to either high- (>median) or low-expression groups. Bottom panels: number of patients at risk, in either stratum, at a given timepoint (unit: day). E, Stable cells expressing LAPTM4B-35-GFP, LAPTM4B-24-GFP, N-terminus-GFP, or GFP; expression in the cell lysates assessed by Western blotting. Left panel: a representative experiment. Right panel: quantification of three experiments, mean ± SEM. F, Real-time measurement of cell migration in cells stably expressing LAPTM4B-35-GFP, LAPTM4B-24-GFP, N-terminus-GFP, or GFP using the xCELLigence system. Those 6×10^4 cells in serum-free medium were seeded in the top chamber; complete medium containing 10% FBS in the lower chamber served as a chemoattractant. Cell migration index measured at an interval of 15 min for 25 h. In five independent experiments, more than 15 wells for each condition were analyzed; mean ± SEM

zebrafish xenograft model at the time we started the current study, here we generated LAPTM4B KO PC-3 cells by CRISPR-Cas9n, which was validated by both sequencing and Western blot (Figure S6A,B). LAPTM4B-35 and LAPTM4B-24 were then stably expressed on the LAPTM4B KO background (Figure S6C,D). Interestingly, compared with WT PC-3 cells, LAPTM4B KO cells displayed reduced wound-healing capability, and this phenotype was rescued by expression of LAPTM4B-35, but not by LAPTM4B-24 (Figure 6A,B), thus

supporting the results obtained with the A431 cell line.[20] Those cell lines we then used to investigate metastatic dissemination in zebrafish. PC-3 cells labeled with a fluorescent dye (CM-DiI) were injected into the perivitelline cavity of embryos at 48 hours post fertilization. These fish were imaged at 36 hours post injection, and cancer cell dissemination was quantified (Figure 6C,D). Compared with that of WT cells, LAPTM4B KO cells had significantly reduced metastatic dissemination that could be rescued by LAPTM4B-35

expression (Figure 6D). These data indicate that LAPTM4B-35 shows prometastatic competence.

3.6 | The current study provides a potential drug target for cancer therapeutics

In the current study, we have shown that LAPTM4B-35 is vital for cell migration and integrin beta1 recycling. To further investigate a potential link between LAPTM4B transcripts expression and metastasis-free survival, we utilized toil-reprocessed[34] expression data from TCGA and GTEx datasets. There are four reported LAPTM4B transcripts in human tissues. Two of these encode both LAPTM4B-35 and -24 (ENST00000619747.1 and ENST00000445593.6; Figure 7A), one has an open reading frame (ORF) for LAPTM4B-24 only (ENST00000521545.6; Figure 7A), and one is a fragment that does not contain a complete ORF for either isoform (ENST00000517924.5).

As LAPTM4B has been associated with poor prognosis in several types of cancers,[35] we investigated whether there is an association between LAPTM4B-35–encoding transcripts and survival in 23 types of cancers found in TCGA (Table S1). High expression of the LAPTM4B-35–encoding transcripts ENST00000619747.1 and ENST00000445593.6 was associated with poor overall survival in five cancers (breast, liver, sarcoma, skin, and thymoma), and the LAPTM4B-24–encoding transcript ENST00000521545.6 alone was associated with poor prognosis in kidney cancers (Table S1). Next, we performed a separate data analysis from skin cancer patients, as this cohort contains sufficiently large amounts of RNAseq data from metastases for a meaningful analysis, and the skin cancer cell line A431 was utilized in most experiments of the current study. The data revealed that high levels of ENST00000619747.1 (LAPTM4B-35–encoding transcript) in the metastatic tumors were associated with poor survival (Figure 7B), while the other transcript variants was not (Figure 7C,D). Finally, we measured LAPTM4B protein in skin cancer patients' tissue samples. Interestingly, in four out of five patients' sample, we found that both LAPTM4B-35 and LAPTM4B-24 expression were upregulation in the tumor tissues, compared with in the noncancerous skin samples (Figure S7A,B).

Due to the distinct difference between the two LAPTM4B isoforms as to cell migration, we next asked whether the LAPTM4B-35–specific N-terminus (N1-91) alone is sufficient to promote cell migration. The N-terminus-GFP expression substantially stimulated cell migration (Figure 7E,F), providing the possibility that N-terminus could prove a novel target for cancer therapy development. Meanwhile LAPTM4B-35-GFP–expressing cells show higher migratory capability than LAPTM4B-24-GFP–expressing cells (Figure 7E,F), in line with the finding by utilizing Flag-tagged cells (Figure S1A,B). We must, however, acknowledge that further studies are crucial to deconvolute the functional structure motif within the LAPTM4B-35–specific N-terminus.

In summary, this study establishes Cdc42 interaction as a novel mechanism of LAPTM4B-35–specific filopodia localization.

Moreover, our data reveal LAPTM4B-35 as stabilizing the filopodia and stimulating downstream FA formation and dynamics, as well as promoting cancer cell dissemination competence. Mechanically, we propose that LAPTM4B-35 regulates integrin beta1 recycling via endosome trafficking.

4 | DISCUSSION

Although several studies have shown a link between LAPTM4B-35 and cancer cell migration,[16,17] the molecular underpinnings of this phenotype are poorly understood. Meanwhile, most studies that address the molecular function of LAPTM4B mainly rely on expression of either one isoform or another. The current study compares the LAPTM4B isoforms by expressing each of them separately on a KO background, confirming previous findings that LAPTM4B-35 can especially stimulate cancer cell migration and metastasis.[15-17,36]

Moreover, this study has established that LAPTM4B-35 partially distributes on filopodia, and we identified Cdc42 as a novel interaction partner for LAPTM4B-35, providing a link between LAPTM4B-35 filopodia localization and enhanced cell migration. Briefly, Cdc42 is an important factor for positioning LAPTM4B-35 to the plasma membrane where it localizes to filopodia, subsequently leading to their stabilization. LAPTM4B-35 further regulates FA dynamics, and, in a zebrafish model, it promotes cancer cell dissemination.

Interestingly, in the current study we found LAPTM4B-35 stabilizes filopodia without affecting Cdc42 activity. Recently, several studies identified proteins regulating filopodia independently of Cdc42 (e.g., LPR1[37] and TRPM2).[38] TRPM2 regulation of filopodia is associated with trafficking of Zn^{2+}-enriched lysosomes to the leading edge of migrating cells, suggesting that lysosome may be involved in the filopodia formation and stabilization by channel functions rather than affecting Cdc42 activity.[38] We anticipate the current study provides a scenario that lysosomal protein may regulate filopodia stabilization via filopodia distribution without affecting Cdc42 activity; however, the detailed molecular mechanism still needs further investigations.

The intercellular trafficking of integrin beta1 is essential for regulating its functions.[26] In this study, we provide evidence that LAPTM4B interacts with integrin beta1, cotraffics on endosomes, and promotes the recycling of integrin beta1.

A report by Milkereit et al.[18] showed that overexpressed LAPTM4B-24 partially distributes to actin-based plasma membrane protrusions in WT HEK-293 cells. Interestingly, in the current study we observed only limited amounts of LAPTM4B-24 in filopodia when expressed on a LAPTM4B KO background. It is plausible that LAPTM4B-24 can in part be recruited to the plasma membrane by interaction with endogenous LAPTM4B-35 in WT cells. In support of this, LAPTM4B has been shown to form oligomers,[39] and here we found that Cdc42 immunoprecipitates endogenous LAPTM4B-35 and -24 in approximately equal amounts from WT cells, although LAPTM4B-24 expressed on a KO background failed to interact with Cdc42.

Here, we report that the LAPTM4B-35–specific N-terminus displays significant promotion of cell migration. Two conserved functional motifs have been identified inside the N-terminus. First, an SH3-domain binding consensus motif (PPRP, amino acids 12-15) has been shown to interact with the p85α regulatory subunit of PI3K to regulate AKT signaling and chemotherapy resistance.[40] Second, a polybasic stretch (8× arginine in amino acids 52-67) can mediate interaction with phosphoinositides and promotes LAPTM4B-35 interaction with the endosomal PIP kinase PIPKIγi5.[41] Recent investigations suggest that phosphoinositides and PIP-binding proteins are enriched in filopodia,[42] which may relate to LAPTM4B-35 distribution and function in these structures. However, it is noteworthy that the common motifs shared in both LAPTM4B isoforms are essential for maintaining protein functions, for example, the conserved C-terminal signals for current lysosomal position,[10,18] the PY motifs necessary for binding the ubiquitin ligase Nedd4,[18] and sphingolipid interaction motif critical for nutrient signaling.[19]

Further studies are necessary to elucidate both the mechanisms that enhance the expression of the oncogenic isoform LAPTM4B-35 and its role in cancer progression.

DISCLOSURE

The authors declare that the research was conducted in the absence of any commercial or financial relationships that could be construed as a potential conflict of interest.

ORCID

Kecheng Zhou https://orcid.org/0000-0003-1753-2524

REFERENCES

1. Hanahan D, Weinberg RA. Hallmarks of cancer: the next generation. *Cell.* 2011;144(5):646-674.
2. Qian C-N, Mei Y, Zhang J. Cancer metastasis: issues and challenges. *Chin J Cancer.* 2017;36(1):38.
3. Mattila PK, Lappalainen P. Filopodia: molecular architecture and cellular functions. *Nat Rev Mol Cell Biol.* 2008;9(6):446-454.
4. Gauthier-Campbell C, Bredt DS, Murphy TH, El-Husseini AE-D. Regulation of dendritic branching and filopodia formation in hippocampal neurons by specific acylated protein motifs. *Mol Biol Cell.* 2004;15(5):2205-2217.
5. Krugmann S, Jordens I, Gevaert K, Driessens M, Vandekerckhove J, Hall A. Cdc42 induces filopodia by promoting the formation of an IRSp53: mena complex. *Curr Biol.* 2001;11(21):1645-1655.
6. Chao W-TT, Kunz J. Focal adhesion disassembly requires clathrin-dependent endocytosis of integrins. *FEBS Lett.* 2009;583(8):1337-1343.
7. Partridge MA, Marcantonio EE. Initiation of attachment and generation of mature focal adhesions by integrin-containing filopodia in cell spreading. *Mol Biol Cell.* 2006;17(10):4237-4248.
8. Vincent M, Jorge L, Guillaume M, et al. Endosomal membrane tension regulates ESCRT-III-dependent intra-lumenal vesicle formation. *Nat Cell Biol.* 2020;22(8):947-959.
9. Tanja M, Hannah S, Daniel FL. On the move: endocytic trafficking in cell migration. *Cell Mol Life Sci.* 2015;72(11):2119-2134.
10. Shao GZ, Zhou RL, Zhang QY, et al. Molecular cloning and characterization of LAPTM4B, a novel gene upregulated in hepatocellular carcinoma. *Oncogene.* 2003;22(32):5060-5069.
11. Ng S, Mitchell A, Kennedy JA, et al. A 17-gene stemness score for rapid determination of risk in acute leukaemia. *Nature.* 2016;540(7633):433-437.
12. Li Y, Zou L, Li Q, et al. Amplification of LAPTM4B and YWHAZ contributes to chemotherapy resistance and recurrence of breast cancer. *Nat Med.* 2010;16(2):214-218.
13. Meng Y, Wang L, Xu J, Zhang Q. AP4 positively regulates LAPTM4B to promote hepatocellular carcinoma growth and metastasis, while reducing chemotherapy sensitivity. *Mol Oncol.* 2018;12(3):373-390.
14. Xiao M, Yang S, Meng F, et al. LAPTM4B predicts axillary lymph node metastasis in breast cancer and promotes breast cancer cell aggressiveness in vitro. *Cell Physiol Biochem.* 2017;41(3):1072-1082.
15. Wang L, Meng Y, Xu J, Zhang Q. The transcription factor AP4 promotes oncogenic phenotypes and cisplatin resistance by regulating LAPTM4B expression. *Mol Cancer Res.* 2018;16(5):857-868.
16. Liu X, Xiong F, Wei X, Yang H, Zhou R. LAPTM4B-35, a novel tetra-transmembrane protein and its PPRP motif play critical roles in proliferation and metastatic potential of hepatocellular carcinoma cells. *Cancer Sci.* 2009;100(12):2335-2340.
17. Yang H, Xiong F, Wei X, Yang Y, McNutt MA, Zhou R. Overexpression of LAPTM4B-35 promotes growth and metastasis of hepatocellular carcinoma in vitro and in vivo. *Cancer Lett.* 2010;294(2):236-244.
18. Milkereit R, Rotin D. A role for the ubiquitin ligase Nedd4 in membrane sorting of LAPTM4 proteins. *PLoS One.* 2011;6(11):e27478.
19. Zhou K, Dichlberger A, Martinez-Seara H, et al. A ceramide-regulated element in the late endosomal protein LAPTM4B controls amino acid transporter interaction. *ACS Cent Sci.* 2018;4(5):548-558.
20. Zhou K, Dichlberger A, Ikonen E, Blom T. Lysosome associated protein transmembrane 4B (LAPTM4B)-24 is the predominant protein isoform in human tissues and undergoes rapid, nutrient-regulated turnover. *Am J Pathol.* 2020;190(10):2018-2028.
21. Vartiainen M, Ojala PJ, Auvinen P, Peränen J, Lappalainen P. Mouse A6/twinfilin is an actin monomer-binding protein that localizes to the regions of rapid actin dynamics. *Mol Cell Biol.* 2000;20(5):1772-1783.
22. Nobes CD, Hall A. Rho, Rac, and Cdc42 GTPases regulate the assembly of multimolecular focal complexes associated with actin stress fibers, lamellipodia, and filopodia. *Cell.* 1995;81(1):53-62.
23. Heckman CA, Plummer HK. Filopodia as sensors. *Cell Signal.* 2013;25(11):2298-2311.

24. Jacquemet G, Baghirov H, Georgiadou M, et al. L-type calcium channels regulate filopodia stability and cancer cell invasion downstream of integrin signalling. *Nat Commun*. 2016;7:13297.

25. Berginski ME, Vitriol EA, Hahn KM, Gomez SM. High-resolution quantification of focal adhesion spatiotemporal dynamics in living cells. *PLoS One*. 2011;6(7):e22025.

26. Caswell P, Norman J. Endocytic transport of integrins during cell migration and invasion. *Trends Cell Biol*. 2008;18(6):257-263.

27. Panicker AK, Buhusi M, Erickson A, Maness PF. Endocytosis of β1 integrins is an early event in migration promoted by the cell adhesion molecule L1. *Exp Cell Res*. 2006;312(3):299-307.

28. Paul NRR, Jacquemet G, Caswell PTT. Endocytic trafficking of integrins in cell migration. *Curr Biol*. 2015;25(22):R1092-R1105.

29. Arjonen A, Alanko J, Veltel S, Ivaska J. Distinct recycling of active and inactive β1 integrins. *Traffic*. 2012;13(4):610-625.

30. Cheng X, Zheng Z, Bu Z, et al. LAPTM4B-35, a cancer-related gene, is associated with poor prognosis in TNM stages I-III gastric cancer patients. *PLoS One*. 2015;10(4):e0121559.

31. Zhang H, Cq W, Liu R, et al. Overexpression of LAPTM4B-35: a novel marker of poor prognosis of prostate cancer. *PLoS One*. 2014;9(3):e91069.

32. Tse BWCC, Volpert M, Ratther E, et al. Neuropilin-1 is upregulated in the adaptive response of prostate tumors to androgen-targeted therapies and is prognostic of metastatic progression and patient mortality. *Oncogene*. 2017;36(24):3417-3427.

33. Teng Y, Xie X, Walker S, White DT, Mumm JS, Cowell JK. Evaluating human cancer cell metastasis in zebrafish. *BMC Cancer*. 2013;13(1):453.

34. Vivian J, Rao AA, Nothaft FA, et al. Toil enables reproducible, open source, big biomedical data analyses. *Nat Biotechnol*. 2017;35(4):314-316.

35. Meng Y, Wang L, Chen D, et al. LAPTM4B: an oncogene in various solid tumors and its functions. *Oncogene*. 2016;35(50):6359-6365.

36. Zhang H, Qi S, Zhang T, et al. miR-188-5p inhibits tumour growth and metastasis in prostate cancer by repressing LAPTM4B expression. *Oncotarget*. 2015;6(8):6092-6104.

37. Sigal YJ, Quintero OA, Cheney RE, Morris AJ. Cdc42 and ARP2/3-independent regulation of filopodia by an integral membrane lipid-phosphatase-related protein. *J Cell Sci*. 2007;120(2):340-352.

38. Li F, Abuarab N, Sivaprasadarao A. Reciprocal regulation of actin cytoskeleton remodelling and cell migration by Ca2+ and Zn2+: role of TRPM2 channels. *J Cell Sci*. 2016;129(10):2016-2029.

39. Vergarajauregui S, Martina JA, Puertollano R. LAPTMs regulate lysosomal function and interact with mucolipin 1: new clues for understanding mucolipidosis type IV. *J Cell Sci*. 2011;124(Pt 3):459-468.

40. Li L, Wei XH, Pan YP, et al. LAPTM4B: a novel cancer-associated gene motivates multidrug resistance through efflux and activating PI3K/AKT signaling. *Oncogene*. 2010;29(43):5785-5795.

41. Tan X, Sun Y, Thapa N, Liao Y, Hedman AC, Anderson RA. LAPTM4B is a PtdIns(4,5)P2 effector that regulates EGFR signaling, lysosomal sorting, and degradation. *EMBO J*. 2015;34(4):475-490.

42. Jacquemet G, Stubb A, Saup R, et al. Filopodome mapping identifies p130Cas as a mechanosensitive regulator of filopodia stability. *Curr Biol*. 2019;29(2):202-216.e7.

SUPPORTING INFORMATION

Additional supporting information may be found in the online version of the article at the publisher's website.